PŮVODNÍ PRÁCE/ORIGINAL PAPER

New occurrence of kruťaite and petříčekite at the former uranium mine Slavkovice, western Moravia, Czech Republic

Tomáš Flégr[1)]*, Jiří Sejkora[2)], Pavel Škácha[2,3)] and Zdeněk Dolníček[2)]

[1)]*Department of Geology, Masaryk University, Kotlářská 267/2, 611 37 Brno; *e-mail:397248@mail.muni.cz*
[2)]*Department of Mineralogy and Petrology, National Museum, Cirkusová 1740, 193 00 Prague 9*
[3)]*Mining Museum Příbram, Hynka Kličky place 293, 261 01 Příbram VI*

Flégr T, Sejkora J, Škácha P, Dolníček Z (2018) New occurrence of kruťaite and petříčekite at the former uranium mine Slavkovice, western Moravia, Czech Republic. Bull Mineral Petrolog 26(2): 250-258. ISSN 2570-7337

Abstract

Two rare copper diselenides, kruťaite and petříčekite, were found in two museum samples of vein fillings from the uranium mine Slavkovice, western Moravia (Czech Republic). Kruťaite occurs as small isometric isolated euhedral to subhedral zoned crystals enclosed and partly replaced by umangite. Petříčekite forms small elongated or isometric inclusions enclosed by kruťaite and other Cu-selenides. Optical data, Raman spectra and chemical composition of both phases are specified in this paper. Kruťaite contains elevated contents of Co (up to 0.15 *apfu*) and Ni (up to 0.09 *apfu*), whereas petříčekite is Ni-Co free and enriched in Fe (up to 0.25 *apfu*). Both phases seem to be the oldest selenides in the given assemblage, and are associated with umangite, athabascaite, eskebornite, klockmannite, bukovite, uraninite, chalcopyrite, calcite and hematite. The studied ore assemblage originated at temperature not exceeding ca. 100 °C. The fugacity of selenium as well as the Se/S ratio of the parent fluids decreased significantly during paragenetic evolution of the studied mineralization.

Key words: *kruťaite, petříčekite, selenides, chemical composition, Raman spectra, uranium deposits, Slavkovice*
Received 12. 6. 2018; accepted 14. 12. 2018

Introduction

Kruťaite, isometric $CuSe_2$, was originally described from the former uranium mine Petrovice, western Moravia (Johan et al. 1972). The mineral is named in honor of mineralogist Dr. Tomáš Josef Kruťa (1906 - 1998) from the Moravian Museum in Brno. Later, occurrences of kruťaite were reported from several localities e. g. El Dragón mine, Bolivia (Grundman et al. 1990), Cacheuta mine, Argentina (Paar et al. 1996), Tumiñico mine, Argentina (Keutsch et al. 2009), Buraco do Ouro gold mine, Brasil (Menez, Botelho 2017), Yutangba deposit, China (Liu et al. 2005) and Weintraube mine, Germany (Sager 1994).

Petříčekite, orthorhombic $CuSe_2$, was recently described from the former uranium mine Předbořice in central Bohemia, El Dragón mine in Bolivia and Sierra de Cacheuta deposit in Argentina (Bindi et al. 2016). Mineral was named after Václav Petříček, renowned crystallographer of the Institute of Physics of the Czech Academy of Sciences, Prague.

In this paper we present new evidence for the presence of kruťaite and petříčekite in ore veins of the Slavkovice uranium deposit, western Moravia, Czech Republic.

History of mining

The uranium deposit Slavkovice was discovered in 1957 and the detailed exploration was done since 1961 to 1964 (Pluskal 1992). The Slavkovice mine is located in NW part of the Slavkovice deposit, whereas its SE part was mined by Petrovice mine (Bajer 1970). During the years 14 fault structures were explored, but economic ore mineralization was proved only in 6 structures, where ore reserves as high as 79 tonnes of uranium in the C_1 category (i.e., indicated ore) and 400 tonnes of U in the C_2 category (i.e., inferred ore) were estimated. Since then, 175 tonnes of uranium were mined out and the mining ceased in 1970 (Sejkora et al. 1997; Pluskal 1992).

Geology and mineralization of the Slavkovice deposit

Former uranium mine Slavkovice is located southwest from Nové Město na Moravě, in the northwest part of the Rožná - Olší ore district, western Moravia, Czech Republic. Ore mineralization is developed in high-grade metamorphic series of the Moldanubian Varied Group. The host rocks include partialy migmatitized or migmatitized biotite paragneisses with lenses of amphibolites, amphibole-biotite gneisses, calc-silicate rocks and marbles (Arapov et al. 1984; Šouba 1974). The deposit belongs to the hydrothermal vein-type uranium deposits with various mineral assemblages, developed in dislocation zones (Šouba 1974). Origin of the Slavkovice uranium deposit is connected with tectonic development in area of the Slavkovice-Škrdlovice shear zone, which is connected to the dominant Labe fault system and minor dislocations of the Křídlo fault (Bajer 1970). Dislocations of the Křídlo fault system crosscut older Labe fault system (Bajer 1970).

The uranium ore deposit is strongly affected by tectonics, which is apparent from the fold structures and fault fissures of the Slavkovice - Škrdlovice shear zone (Šouba 1974). Ore veins and ore zones of the Slavkovice deposit are divided according to their morphology into zone dislocations, moderately dipped veins and steep veins (Bajer

1970). Zone dislocations are 2 - 40 m thick, have strikes 280 - 330° and dip 25 - 80° to the northeast. They are filled up with tectonically crushed and altered rocks; carbonate veins also occur in places (Bajer 1970). The moderately dipped veins dip 15 - 45° to the northeast, their directions follow Labe fault system and their lengths reach up to 2 km. The moderately dipped veins are filled up with tectonically crushed rocks and carbonate gangue containing uranium mineralization (Bajer 1970). The steep veins are the most abundant type represented by carbonate veins carrying all stages of the mineralization. They strike W - E to WNW - ESE and dip steeply (60 - 90°) to the N. Their thickness is 0.5 - 1 m and it decreases as the veins run away of contact with moderately dipped veins (Bajer 1970).

The veins and dislocation zones of the Slavkovice deposit are filled up by the quartz - carbonate - uraninite mineralization (Kvaček 1973; Šouba 1974). Šouba (1974) defined three hypogene mineralization stages. First stage is formed by quartz I, second stage includes dolomite and quartz II and third stage is characterized by the carbonate-uraninite assemblage. The most widespread is the last stage which can be further divided into oxide, selenide and sulphide substages (Šouba 1974).

Hydrothermal ore minerals uraninite, hematite, goethite, sulphides and selenides occurred in the Slavkovice deposit. Uraninite forms typical collomorphic aggregates, which are affected by dissolution and replacement by younger minerals including carbonates, hematite, goethite, selenides and sulphides (Šouba 1974). Selenides are typically present as disseminated grains and aggregates of crystals in the uraninite in close relationship with oxides and sulphides. The most abundant selenide minerals are umangite, eskebornite and clausthalite, however also berzelianite, bukovite, klockmannite, ferroselite, eucairite, naumannite and tyrrellite are present (Kvaček 1969; Šouba 1974).

Table 1 *Reflectance values of kruťaite from Slavkovice*

λ (nm)	R (%)
400	35.90
420	36.85
440	36.97
460	36.71
480	36.70
500	36.49
520	36.04
540	35.41
560	34.77
580	34.03
600	33.26
620	32.56
640	32.07
660	31.54
680	31.53
700	31.67

Methods

The selenide mineralization from Slavkovice was studied in fragments of the carbonate vein fillings cut from two samples deposited in collections of the Moravian Museum in Brno. Optical properties of ore minerals observed in polished sections were studied in the reflected light, using polarizing microscope Nicon Eclipse ME600 equipped by Nikon DXM 1200F digital camera (National Museum, Prague). Reflectance measurements for kruťaite and petříčekite were obtained in air relative to a

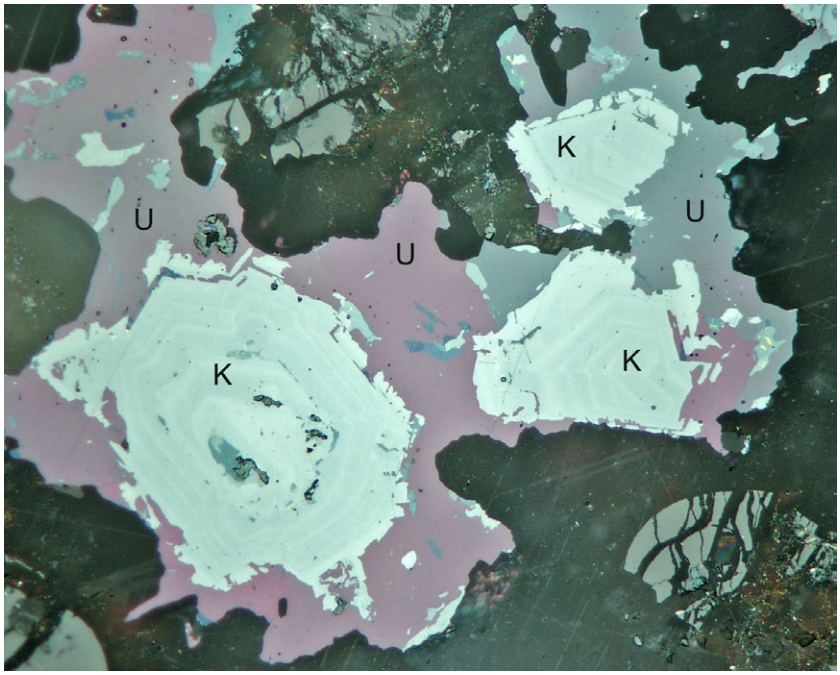

Fig. 1 *Three zonal crystals of kruťaite (K) in the aggregates of umangite (U), Slavkovice; field of view 270 μm; photo (T. Flégr) in reflected light.*

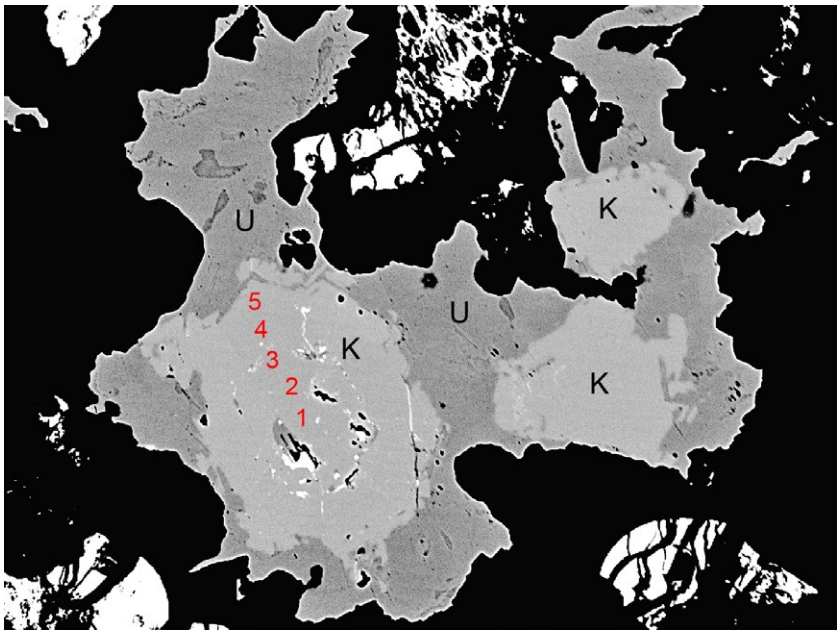

Fig 2 *Same photo as Fig. 1; kruťaite (K) in umangite (U); red numbers indicate point analyses in zonal kruťaite crystal, Slavkovice; field of view 300 μm; BSE photo (T. Flégr).*

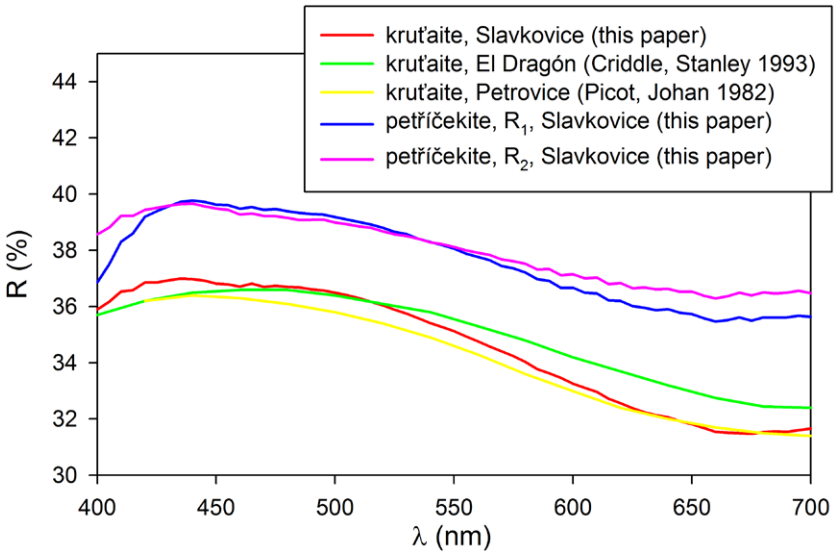

Fig. 3 *Reflectance curves for kruťaite and petříčekite from Slavkovice in comparison with published data.*

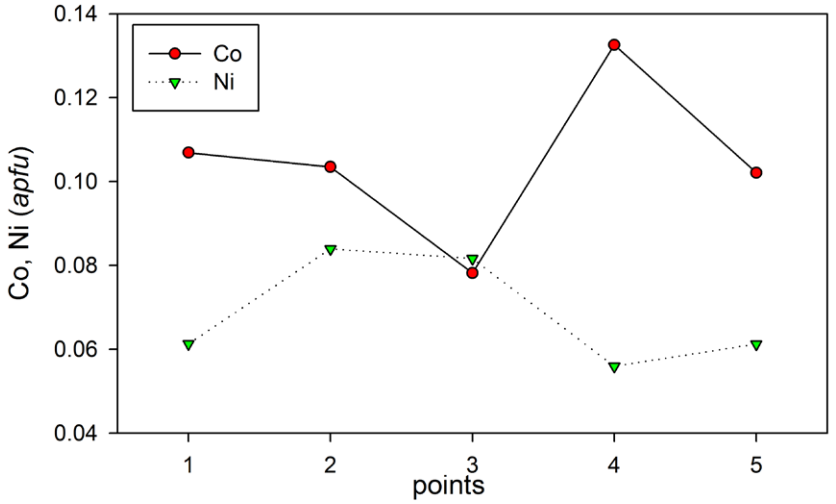

Fig. 4 *Variation of Co and Ni contents (apfu) in zonal kruťaite crystal (for position of points see Fig. 2).*

WTiC standard (Zeiss 370) by means of a MSP400 TIDAS spectrometer using objective 100x on a Leica ore microscope.

Afterwards the chemical analyses were performed using a Cameca SX 100 electron microprobe (National museum, Prague) operating in the WDS mode (25 kV, 20 nA and 2 μm wide beam). The following standards and X-ray lines were used to minimize line overlaps: Ag (AgLα), Au (AuMα), Bi (BiMβ), CdTe (CdLα), Co (CoKα), chalcopyrite (CuKα), FeS_2 (FeKα, SKα), HgTe (HgMα), NiAs (NiKα, AsLα), PbS (PbMα), PbSe (SeLα), PbTe (TeLα), Sb_2S_3 (SbLα), Tl(Brl) (TlLα), ZnS (ZnKα), Sn (SnLα), Ge (GeLα) and Pd (PdLα). Peak counting times were 20 s for all elements, and one half of the peak time for each background. Elements, which are not included in the tables, were found to be below the detection limits (0.02 - 0.05 wt. %) in all cases. Raw intensities were converted to the concentrations of elements using automatic *„PAP"* (Pouchou, Pichoir 1985) matrix-correction software.

Raman spectra of the studied samples of kruťaite and petříčekite (grains in a polished section) were collected at room temperature in the range 38 - 2015 cm^{-1} using a DXR dispersive Raman Spectrometer (Thermo Scientific) mounted on confocal Olympus microscope. The Raman signal was excited by an unpolarized 633 nm He-Ne laser and detected by a CCD detector. The experimental parameters were: 100x objective (estimated diameter of the

Table 2 *Representative chemical analyses of kruťaite from Slavkovice (wt. %)*

	1	2	3	4	5	6	7	8	9	10	11	12	13	14	15
Ag	0.00	0.14	0.00	0.00	0.00	0.00	0.00	0.00	0.00	0.00	0.26	0.06	0.00	0.05	0.12
Fe	0.00	0.13	0.07	0.00	0.00	0.00	0.00	0.00	0.00	0.07	0.93	0.40	0.90	1.55	0.29
Ni	1.63	2.24	2.18	1.50	1.64	1.67	2.11	1.85	2.31	1.03	1.58	2.24	2.47	1.75	2.51
Co	3.08	2.99	2.26	3.85	2.96	2.50	4.28	2.74	4.09	2.88	2.66	2.68	1.85	1.79	2.01
Cu	24.00	23.75	24.31	23.75	24.54	24.39	21.97	24.14	22.12	25.02	24.15	22.91	23.77	25.22	24.56
Se	71.58	71.19	71.73	71.83	71.73	71.78	71.81	71.87	71.83	71.67	70.53	72.80	71.95	72.02	72.01
S	0.00	0.00	0.00	0.04	0.00	0.00	0.06	0.03	0.05	0.00	0.00	0.08	0.00	0.00	0.00
total	100.29	100.44	100.55	100.97	100.87	100.34	100.23	100.63	100.40	100.67	100.11	101.17	100.94	102.38	101.50
Ag	0.000	0.003	0.000	0.000	0.000	0.000	0.000	0.000	0.000	0.000	0.005	0.001	0.000	0.001	0.002
Fe	0.000	0.005	0.003	0.000	0.000	0.000	0.000	0.000	0.000	0.003	0.037	0.016	0.035	0.060	0.011
Ni	0.061	0.084	0.082	0.056	0.061	0.063	0.079	0.069	0.087	0.039	0.059	0.083	0.092	0.064	0.093
Co	0.107	0.103	0.078	0.133	0.102	0.087	0.149	0.095	0.142	0.100	0.092	0.092	0.064	0.061	0.069
Cu	0.833	0.822	0.841	0.818	0.846	0.846	0.762	0.835	0.766	0.865	0.838	0.788	0.818	0.853	0.841
Σ cat	1.001	1.017	1.004	1.006	1.009	0.996	0.990	0.998	0.994	1.007	1.029	0.980	1.009	1.039	1.016
Se	1.999	1.983	1.997	1.991	1.991	2.004	2.006	1.999	2.002	1.994	1.969	2.014	1.992	1.961	1.984
S	0.000	0.000	0.000	0.003	0.000	0.000	0.004	0.002	0.003	0.000	0.000	0.005	0.000	0.000	0.000
Se+S	1.999	1.983	1.997	1.994	1.991	2.004	2.010	2.002	2.006	1.994	1.969	2.020	1.992	1.961	1.984
apfu on the base = 3															

laser spot less than 1 μm), 10 s exposure time, 100 exposures, 1200 lines/mm grating (spectral resolution better than 4 cm^{-1}), 50 μm slit spectrograph aperture and 2 mW laser power level. The spectra were repeatedly acquired from different grains in order to obtain a representative spectrum with the best signal-to-noise ratio. The eventual thermal damage of the measured point was excluded by visual inspection of excited surface after measurement, by observation of possible decay of spectral features in the start of excitation and checking for thermal downshift of Raman lines. The instrument was set up by a software-controlled calibration procedure using multiple neon emission lines (wavelength calibration), multiple polystyrene Raman bands (laser frequency calibration) and standardized white-light sources (intensity calibration). Spectral manipulations were performed using the Omnic 9 software (Thermo Scientific).

Kruťaite

Kruťaite was found to be minor component of selenide mineralization in both studied samples. It forms individual isometric hypautomorphic to xenomorphic crystals up to 100 μm in size, enclosed in and partly also corroded by irregularly shaped aggregates of umangite, which are sometimes rimmed by eskebornite (Figs. 1 and 2). In reflected light, kruťaite crystals often display distinct concentric zonation, striking from light blue to light gray colour with slightly different reflectance in various growth zones. The growth zoning can be sometimes highlighted by enclosed minute inclusions of uraninite or calcite, or by selective replacement of certain zones by younger Cu selenides (umangite, klockmannite, athabascaite). Under crossed polars, all grains/growth zones of the studied kruťaite seem to be isotropic. The observed zonation is probably caused by some variations of the chemical composition (see below). Similar zonation of kruťaite was reported from the Petrovice deposit (Kvaček 1979), but in Petrovice the kruťaite is replaced by younger claustalite (Kvaček 1979). The reflectance values for the studied kruťaite (Table 1) are very close to the published data for Ni-Co bearing kruťaite from Petrovice and El Dragón mine (Fig. 3).

According to chemical analyses (Table 2), the cation position of kruťaite shows next to the dominant Cu (0.76-0.87 *apfu*) minor substitution of Co (0.07 - 0.16 *apfu*) and Ni (0.04 - 0.09 *apfu*), locally also elevated contents of Fe (up to 0.06 *apfu*) were detected. The observed optical zonation (Fig. 1) is caused by variation of Co and Ni contents without mutual correlation (Fig. 4). Kruťaite from Petrovice (Johan et al. 1972) shows similar composition with less Cu (0.74 *apfu*) and slightly more trogtalite (up to 0.20 *apfu* Co) and penroseite (up to 0.17 *apfu* Ni) components (Fig. 5), with only traces of Fe (up to 0.03 *apfu*). In the anion site of kruťaite from Slavkovice, the dominant Se is locally substituted by S only in a very minor range (up to 0.01 *apfu*).

The experimental Raman spectrum of kruťaite from Slavkovice (Fig. 6) corresponds very well with spectra of this mineral phase from El Dragón mine, Bolivia - R060381 at RRUFF database (Lafuente et al. 2015) and those for synthetic isometric $CuSe_2$ (Anastassakis 1973). A broad band at 515 cm^{-1} is attributed to the second-order overtone, the strong band at 245 cm^{-1} with shape component at 260 cm^{-1} were assigned to Se-Se stretching vibration and band at 125 cm^{-1} is connected to Cu-Se_2 librations (Anastassakis 1973; Vogt et al. 1983; Lutz, Müller 1991). Weak bands below 100 cm^{-1} should correspond to external and lattice modes.

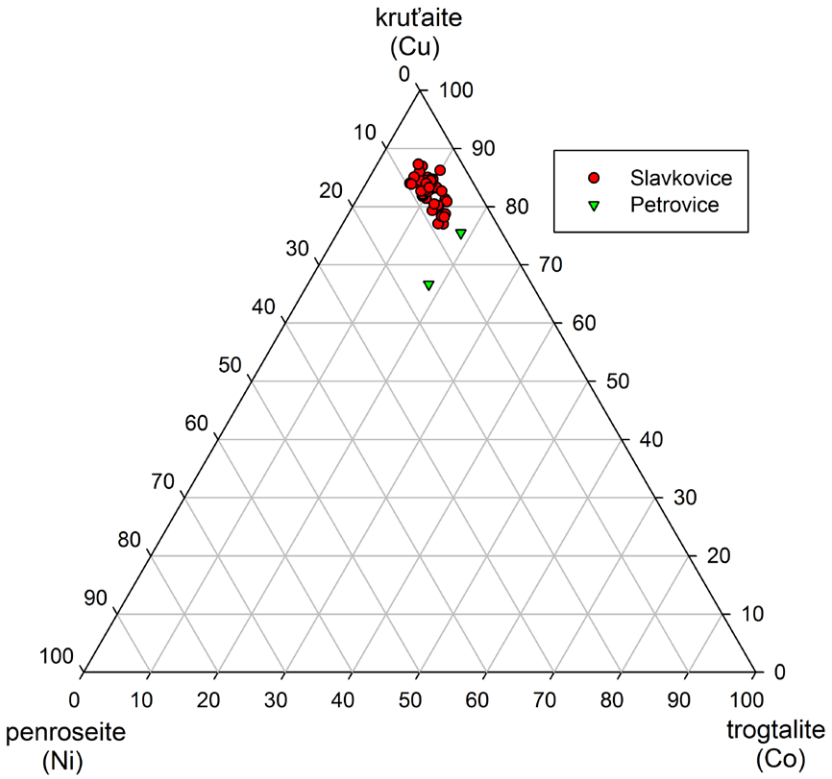

Fig. 5 *Ternary diagram showing distribution between Cu, Co and Ni in kruťaite from Petrovice (Johan et al. 1972) and Slavkovice (this paper).*

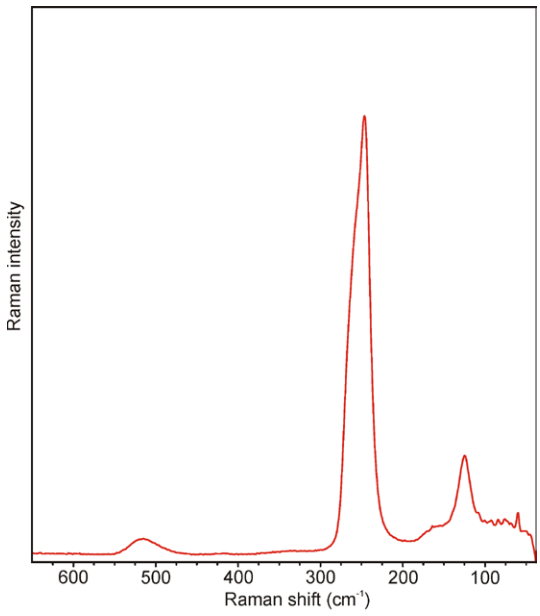

Fig. 6 *Raman spectrum of kruťaite from Slavkovice.*

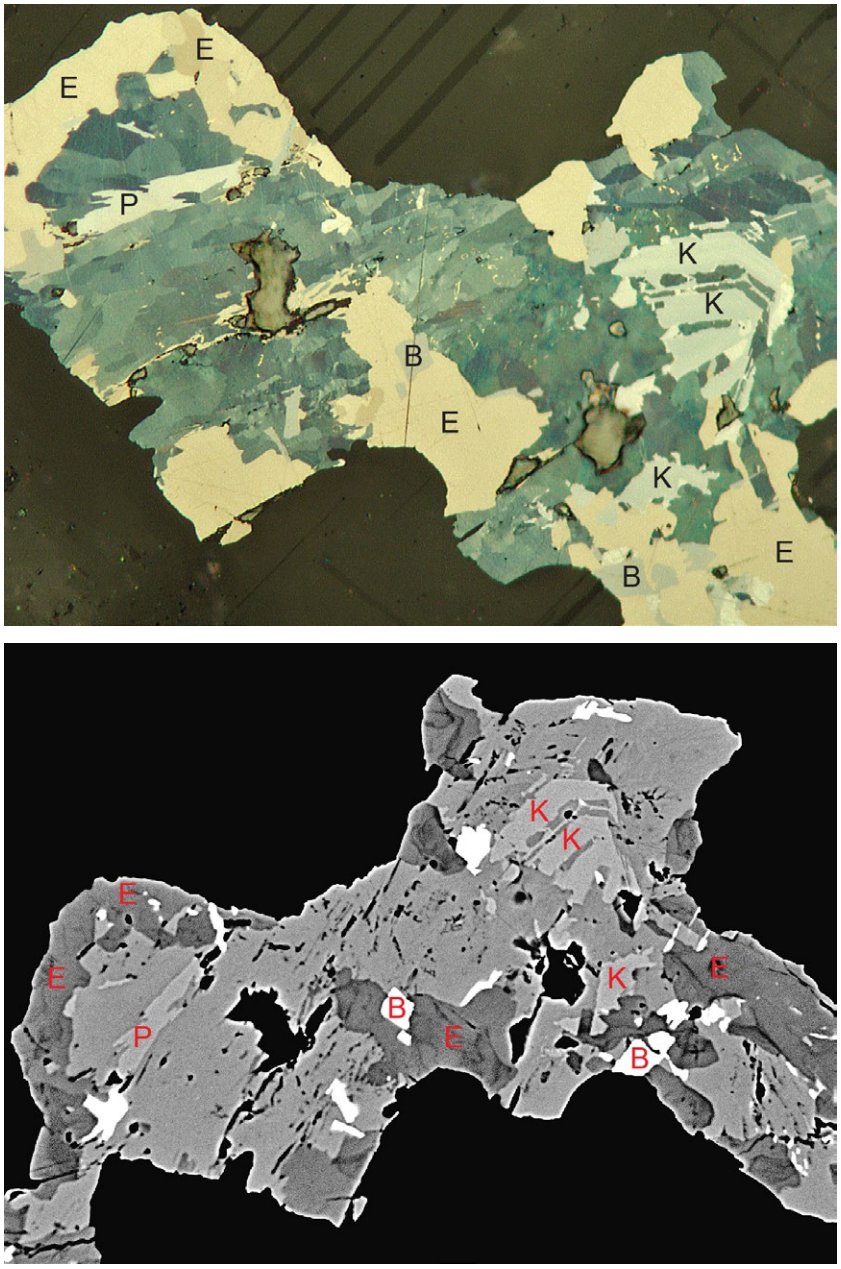

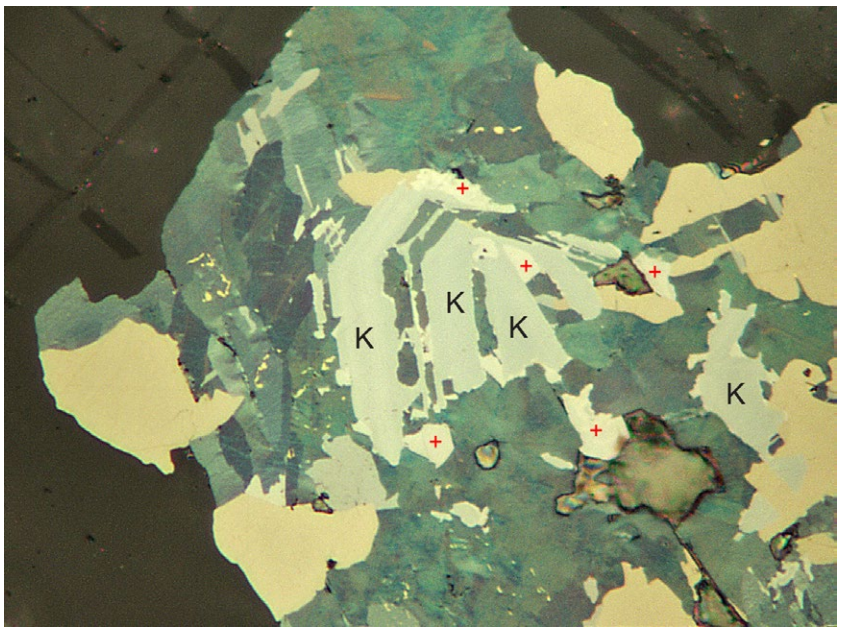

Petříčekite

Petříčekite was observed very sporadically. It forms elongated or isometric subhedral to anhedral individual crystals up to 30 μm in length, which are enclosed in kruťaite or other Cu-selenides (Figs. 7 and 8). In reflected light, petříčekite crystals show distinctly higher reflectivity than neighbouring kruťaite (Fig. 9). Petříčekite is slightly anisotropic, showing weak pleochroism in white-grey tints and grey polarizing colours. The extinction is parallel with respect to elongation of crystals. No apparent zonality of crystals is observed in both polarizing microscope and BSE images. Its measured reflectance values (Table 3) distinctly differ from kruťaite ones and reflect higher reflectivity and anisotropic character of this mineral (Fig. 3). Comparison with published reflectance data of petříčekite from Předbořice and El Dragón mine (Bindi et al. 2016) is not possible because published data for both occurrences are significantly different (probably due to their varied Fe contents).

Fig. 7 *Mineral assemblage of selenides from Slavkovice; isolated crystals of kruťaite (K) and petříčekite (P) in aggregates of klockmannite (bluish grey aggregates with strong anisotropy) rimmed by eskebornite (E) with grains of bukovite (B); field of view 210 μm; photo (Z. Dolníček) in reflected light.*

Fig. 8 *BSE image (Z. Dolníček) of the same ore aggregate as in Fig. 7; K - kruťaite, P - petříčekite, E - eskebornite, B - bukovite; main grey aggregate is klockmannite; note the same grey tint of both $CuSe_2$ polymorphs despite their differences in chemical composition.*

Fig. 9 *Detail of Figs. 7 - 8 showing zoned slightly corroded crystal of kruťaite (K) containing small inclusions of petříčekite (red cross) with higher reflectivity; field of view 100 μm; photo (Z. Dolníček) in reflected light.*

Table 3 *Reflectance values of petříčekite from Slavkovice*

λ (nm)	R_1 (%)	R_2 (%)
400	36.87	38.56
420	39.19	39.44
440	39.77	39.67
460	39.48	39.27
480	39.39	39.15
500	39.19	38.99
520	38.80	38.68
540	38.29	38.28
560	37.77	37.92
580	37.20	37.51
600	36.67	37.15
620	36.20	36.84
640	35.91	36.64
660	35.47	36.29
680	35.62	36.51
700	35.63	36.47

Table 4 *Chemical composition of petříčekite from Slavkovice (wt. %)*

	mean	1	2
Fe	6.36	6.56	6.15
Cu	22.88	22.73	23.03
Se	72.11	72.12	72.10
S	0.10	0.12	0.07
total	101.44	101.53	101.35
Fe	0.246	0.253	0.238
Cu	0.777	0.771	0.783
Σ cat	1.023	1.024	1.021
Se	1.971	1.968	1.974
S	0.006	0.008	0.005
Se+S	1.977	1.976	1.979
apfu on the base = 3			

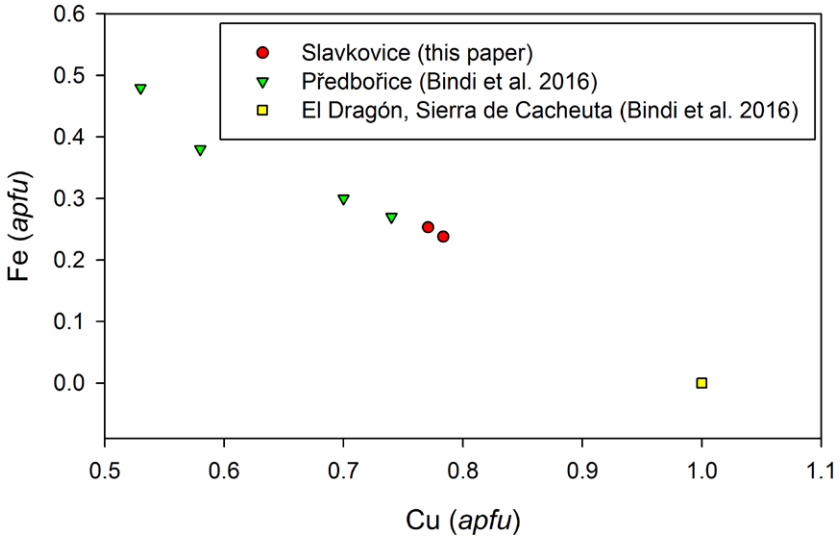

Fig. 10 *Graph of Cu vs Fe contents (apfu) for petříčekite.*

Chemical composition of petříčekite from Slavkovice (Table 4) is rather simple. In contrast with associated kruťaite, petříčekite is Co- and Ni-free and beside dominant Cu (0.77 - 0.78 *apfu*) contains only 0.24 - 0.25 *apfu* Fe (Fig. 10). In the anion site, dominant Se is substituted by S in a trace range (up to 0.01 *apfu*). Its average empirical formula (mean of 2 analyses) on the basis of 3 *apfu* is $(Cu_{0.78}Fe_{0.25})_{\Sigma 1.03}(Se_{1.97}S_{0.01})_{\Sigma 1.98}$.

The Raman spectrum of petříčekite (Fig. 11) is significantly different from kruťaite one (Fig. 6); this confirms Raman spectroscopy as a very useful tool for distinction of polymorphic modifications. The more complex character of experimental spectrum is probably caused by lower symmetry of petříčekite but tentative assigment of both spectra is similar (Anastassakis 1973; Vogt et al. 1983; Lutz, Müller 1991). A weak and broad band at 483 cm^{-1} is assigned to the second-order overtone, the strong band at 230 cm^{-1} with medium strong bands at 275 and 245 cm^{-1} were attributed to Se-Se stretching vibration and bands at 186, 173, 152, 128 and 126 cm^{-1} are probably connected to Cu-Se_2 librations. A weak bands below 100 cm^{-1} should correspond to external and lattice modes.

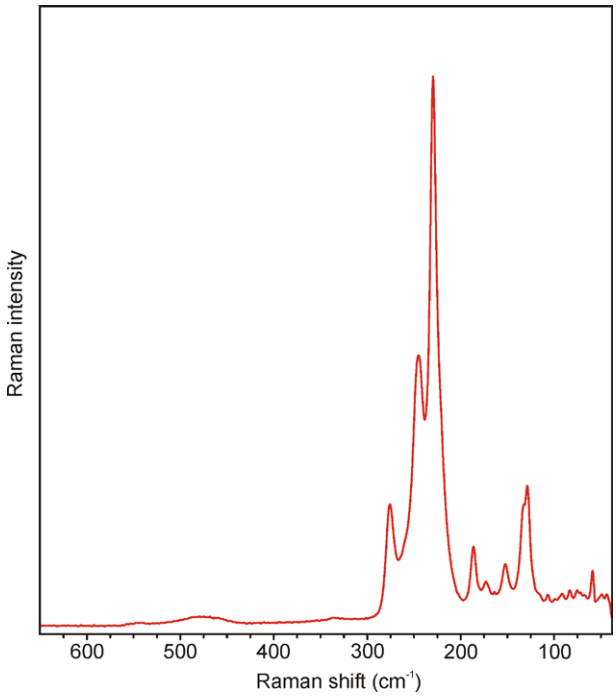

Fig. 11 *Raman spectrum of petříčekite from Slavkovice.*

Table 5 *Chemical composition of Cu selenides from Slavkovice (wt. %)*

	klockmannite					athabascaite			umangite					
	1	2	3	4	5	1	2	3	1	2	3	4	5	6
Ag	0.00	0.08	0.05	0.00	0.00	0.00	0.00	0.00	0.00	0.00	0.00	0.00	0.00	0.00
Fe	0.09	0.58	0.25	1.03	0.00	0.31	0.19	0.00	0.00	0.00	0.00	0.00	0.22	0.23
Cu	43.31	43.33	44.40	43.65	44.56	51.00	51.13	52.16	54.31	54.57	54.55	54.22	54.15	54.72
Se	56.13	56.17	55.31	55.06	53.74	45.69	45.42	47.10	45.23	44.48	43.47	43.73	43.37	43.51
S	0.22	0.13	0.38	0.47	0.29	1.99	1.78	0.97	0.42	0.49	0.85	0.21	0.37	0.40
total	99.75	100.29	100.39	100.21	98.59	98.99	98.52	100.23	99.96	99.54	98.87	98.16	98.11	98.86
apfu	2	2	2	2	2	9	9	9	5	5	5	5	5	5
Ag	0.000	0.001	0.001	0.000	0.000	0.000	0.000	0.000	0.000	0.000	0.000	0.000	0.000	0.000
Fe	0.002	0.015	0.006	0.026	0.000	0.034	0.021	0.000	0.000	0.000	0.000	0.000	0.014	0.014
Cu	0.973	0.968	0.987	0.969	1.008	4.985	5.033	5.103	2.966	2.987	2.990	3.018	3.007	3.014
Se	1.015	1.010	0.989	0.984	0.979	3.595	3.598	3.709	1.988	1.960	1.918	1.959	1.938	1.928
S	0.010	0.006	0.017	0.021	0.013	0.386	0.347	0.188	0.045	0.053	0.092	0.023	0.041	0.044
Se+S	1.025	1.016	1.006	1.005	0.992	3.980	3.946	3.897	2.034	2.013	2.010	1.982	1.979	1.972
cat/an	0.95	0.97	0.99	0.99	1.02	1.26	1.28	1.31	1.46	1.48	1.49	1.52	1.53	1.54

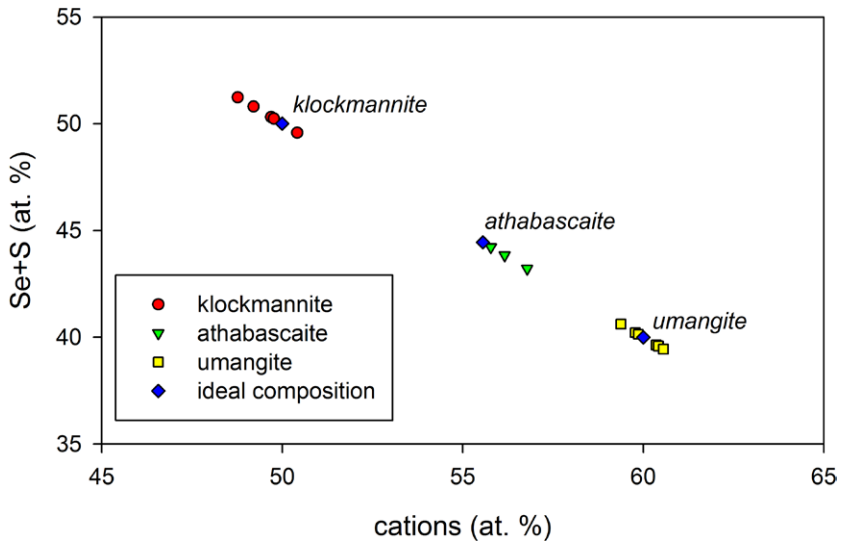

Fig. 12 *Graph of cations vs. Se+S contents (at. %) for klockmannite, athabascaite and umangite from Slavkovice.*

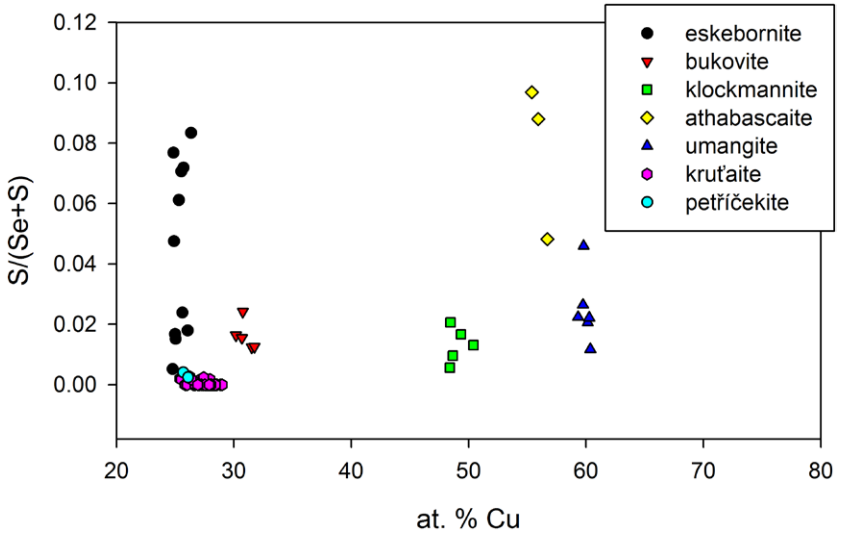

Fig. 13 *The plot at. % Cu vs. S/(S+Se) showing range of SSe_{-1} substitution in the studied selenides.*

Associated selenides

Umangite and eskebornite are the dominant selenide phases in the studied mineralization. Both minerals usually form xenomorphic aggregates randomly growing through each other, both are up to 1 mm in size. Their aggregates are often covered by younger xenomorphic crystals or aggregates of hematite. Nevertheless the umangite predominates over eskebornite. Athabascaite is rarely observed in association with umangite and eskebornite, forming xenomorphic crystals up to 100 μm in size. The eskebornite is associated with klockmannite, which is less abundant but still present in significant amounts, forming irregularly shaped, xenomorphic crystals and zones in the crystals of eskebornite not exceeding 150 μm in size. Both eskebornite and klockmannite enclose relatively often grains of bukovite (Fig. 7 and 8), which forms narrow ledge-shaped crystals growing through them or developed along grain boundaries of them. It is noteworthy that umangite is only rarely observed in the association with aggregates of eskebornite, klockmannite and bukovite as grains reaching 50 μm in size. The crystals of umangite and eskebornite are also sporadically penetrated by small veinlets of younger chalcopyrite, which reach up to 10 μm in thick.

In general, the whole studied association of selenides is dominant by Cu and Se with only low contents of S. Study of the chemical composition of umangite as the most abundant associated phase (Table 5) confirmed minor contents of Fe (up to 0.01 *apfu*)

Table 6 *Chemical composition of eskebornite from Slavkovice (wt. %)*

	1	2	3	4	5	6	7	8	9	10	11
Fe	20.04	20.84	20.61	19.50	20.06	19.42	19.39	19.80	18.94	19.26	20.84
Cu	22.94	23.30	25.15	22.50	23.06	23.83	23.65	23.57	23.99	22.72	24.33
Se	56.10	53.55	53.30	56.89	55.29	54.74	56.49	54.85	56.71	56.53	53.71
S	0.35	1.81	1.97	0.12	1.12	1.69	0.56	1.45	0.42	0.39	1.69
total	99.43	99.50	101.03	99.01	99.53	99.68	100.09	99.67	100.06	98.90	100.57
Fe	0.996	1.012	0.983	0.978	0.986	0.947	0.956	0.968	0.937	0.964	1.002
Cu	1.002	0.995	1.054	0.992	0.996	1.021	1.025	1.013	1.043	1.000	1.029
Se	1.972	1.840	1.799	2.019	1.922	1.888	1.971	1.896	1.984	2.002	1.827
S	0.030	0.153	0.164	0.010	0.096	0.144	0.048	0.123	0.036	0.034	0.142
S+Se	2.002	1.993	1.962	2.029	2.018	2.032	2.019	2.020	2.020	2.036	1.969
apfu on the base = 4											

in addition to dominant Cu; the anion site is occupied by Se with only minor contents of S (0.02 - 0.09 *apfu*). The average empirical formula of the studied umangite from the Slavkovice deposit (mean of 6 analyses) on the basis of 5 *apfu* is $Cu_{3.00}(Se_{1.95}S_{0.05})_{\Sigma 2.00}$.

During the study of chemical composition of klockmannite (Table 5) increased Fe contents (up to 0.03 *apfu*) and traces of Ag were observed; the cation/anion ratio varies in the range 0.95 - 1.02 (Fig. 12) probably due to intergrowth with other Cu-selenides on a sub-microscopic scale (similar as described from other occurrences e.g. by Sejkora et al. 2012, 2014; Škácha et al. 2017). In the anion site, dominant Se is substituted by S in a minor range (up to 0.02 *apfu*). The empirical formula of klockmannite (average of 5 analyses) on the basis of 2 *apfu* is $(Cu_{0.98}Fe_{0.01})_{\Sigma 0.99}(Se_{1.00}S_{0.01})_{\Sigma 1.01}$.

The chemical composition of athabascaite (Table 5) is represented by cation/anion ratio in the range 1.26 - 1.31 (Fig. 12). The studied aggregates are possibly formed by very fine intergrowths with other Cu selenides and this may be the reason for observed non-stoichiometry. Similar situation is known for athabascaite from other occurrences (Sejkora et al. 2012; Škácha et al. 2017). The cation part of the formula contains locally Fe (up to 0.03 *apfu*) in addition to dominant Cu. The anion part features a minor SeS_{-1} substitution; sulphur contents attain up to 0.39 *apfu*; contents of sulphur in athabascaite are higher than in other studied selenides (Fig. 13). The average empirical formula of the studied athabascaite (mean of 3 analyses) on the basis of 9 *apfu* is $(Cu_{5.04}Fe_{0.02})_{\Sigma 5.06}(Se_{3.64}S_{0.31})_{\Sigma 3.95}$.

The chemical composition of eskebornite is simple and close to the ideal formula $CuFeSe_2$; only S contents in the range 0.01 - 0.16 *apfu* were determined (Table 6). The empirical formula of eskebornite (mean of 13 analyses), based on 4 *apfu* is $Cu_{1.02}Fe_{0.98}(Se_{1.92}S_{0.08})_{\Sigma 2.00}$.

The chemical composition of bukovite is also simple (Table 7); only traces of Ag (up to 0.01 *apfu*) and minor contents of S (up to 0.09 *apfu*) were identified locally. Based on 10 *apfu*, its chemical composition (average of 5 analyses) can be expressed by the empirical formula $Cu_{3.10}Fe_{1.02}Tl_{1.87}(Se_{3.95}S_{0.06})_{\Sigma 4.01}$.

Discussion and conclusion

New occurrence of two rare copper diselenides, kruťaite and petříčekite, was found in vein mineralization from the former uranium mine Slavkovice. Both polymorphs were distinguished due to their different optical properties, Raman spectra and chemical composition.

Kruťaite and petříčekite seem to represent the oldest selenides in the studied paragenesis. Both phases are rimmed and partly also replaced by other Cu-selenides and eskebornite. Based on textural evidence, the following paragenetic sequence of ore minerals can be reconstructed: uraninite → kruťaite/petříčekite → umangite → klockmannite → eskebornite → chalcopyrite.

Table 7 *Chemical composition of bukovite from Slavkovice (wt. %)*

	1	2	3	4	5
Ag	0.08	0.00	0.06	0.00	0.00
Fe	5.87	5.53	6.19	5.95	6.27
Co	0.00	0.07	0.00	0.00	0.00
Tl	39.88	39.81	39.49	39.58	41.37
Cu	19.77	21.10	21.46	20.34	20.55
Se	32.52	33.23	32.84	32.85	31.80
S	0.22	0.17	0.17	0.21	0.32
total	98.34	99.91	100.21	98.93	100.31
Ag	0.007	0.000	0.005	0.000	0.000
Fe	1.020	0.940	1.042	1.022	1.068
Co	0.000	0.010	0.000	0.000	0.000
Tl	1.893	1.850	1.817	1.857	1.926
Cu	3.018	3.153	3.175	3.069	3.078
Se	3.995	3.996	3.911	3.989	3.833
S	0.067	0.050	0.050	0.063	0.095
Se+S	4.062	4.047	3.960	4.052	3.928
apfu on the base = 10					

The presence of umangite and absence of berzelianite in the studied paragenesis suggest formation temperatures below 112 °C (Simon, Essene 1996). Similarly, the local occurrence of athabascaite indicates temperatures below 100 °C (Harris et al. 1970).

The presence of hematite indicates highly oxidizing conditions (above magnetite/hematite buffer) during precipitation of ore minerals. The high fugacity of oxygen is suggested also from very low extent of SeS_{-1} substitution in selenides (Simon, Essene 1996). The S/(Se+S) of kruťaite and petříčekite is always lower than 0.005, those for bukovite, klockmannite and umangite range between 0.01 and 0.03, for athabascaite and eskebornite mostly between 0.05 and 0.10 (Fig. 13), and for the veinlets of chalcopyrite (though not analysed quantitatively) it is already above 0.50. As indicated above, the paragenetic evolution occurred in the essentially same sequence. Therefore, a systematic increase of S/Se ratio associated with probable decrease of oxygen fugacity occurred during the crystallization of the studied mineralization.

Assuming the crystallization temperature of 100 °C, the fSe_2 of the parent fluids decreased over three orders of magnitude during crystallization of early portion of selenide assemblage only, from ca. $10^{-11.5}$ (kruťaite stable) to ca. $10^{-14.5}$ (umangite stable). During crystallization of late chalcopyrite, the fS_2 of the parent fluids increased significantly as it could range between ca. 10^{-25} (assemblage hematite + berzelianite unstable) and 10^{-17} (assemblage bornite + pyrite unstable); cf. Simon et al. (1997).

Acknowledgements

The research of selenides from Slavkovice was financially supported by internal grant of National Museum, Prague. Further support was provided by the long-term project DKRVO 2018/02 of the Ministry of Culture of the Czech Republic (National Museum, 00023272).

References

Anastassakis E (1973) Light scattering in transition metal diselenides $CoSe_2$ and $CuSe_2$. Solid State Comm 13: 1297-1301

Arapov JA, Afanasjev GV, Badár J, Bajuškin IM, Blažek J, Bojcov VJ, Bošina B, Brodin BV, Černeceva KN, Česnokov NI, Dančev VI, Dědič K, Djakonov AV, Doležel M, Fiala V, Habásko J, Hájek A, Halbrštát J, Hrádek J, Hřebec J, Ivanov KE, Jakovjenko AM, Jegorov V S, Kolář M, Kolek M, Komínek J, Kozyrev VN, Kremčukov VA, Lažanský M, Lepka F, Malyšev VI, Melnik IG, Měščerskij IM, Milovanov IA, Nikulin VP, Novik-Kačan VP, Nový V, Obr F, Ordynec GE, Petroš R, Portnov FK, Prokeš S, Prokop L, Romanidis K, Saveljeva KT, Stafějev KG, Steiner J, Šorf F, Veselý T, Vilhelm S, Zavarzin AV, Zinověv GD, Zontov NS, Žukova VI (1984) Československá ložiska uranu. Československý uranový průmysl, Praha, 350 pp

Bajer B (1970) Strukturně tektonické poměry ložiska Slavkovice. Symposium pracovníků báňského průmyslu. Hornická Příbram ve vědě a technice sekce Geologie rudních ložisek: 1-31

Bindi L, Förster HJ, Grundmann G, Keutsch FN, Stanley CJ (2016) Petříčekite, $CuSe_2$, a new member of the marcasite group from the Předbořice Deposit, Central Bohemia Region, Czech Republic. Minerals 6, 33

Criddle AJ, Stanley CJ (1993) Quantitative Data File for Ore Minerals. Chapman & Hall, London 635 pp

Grundman G, Lehrberger G, Günter SK (1990) The El Dragón Mine, Potosí, Bolivia. Mineral Record 21: 133-146

Harris DC, Cabri LJ, Kaiman S (1970) Athabascaite: a new copper selenide from Martin Lake, Saskatchewan. Can Mineral 10: 207-215

Johan Z, Picot P, Roland P, Kvaček M (1972) La kruťaite $CuSe_2$, un noveau minéral du grupe de la pyrite. Bull Soc fr Mineral Cristallogr 95: 475-481

Keutsch FN, Förster H-J, Stanley CJ, Rhede D (2009) The discreditation of hastite, the orthorhombic dimorph of $CoSe_2$, and observations on trogtalite, cubic $CoSe_2$, from the type locality. Can Mineral 47: 969-976

Kvaček M (1969) Selenidy uranových ložisek Českomoravské vrchoviny. MS, Kandidátská disertační práce. Ústav nerostných surovin. Kutná Hora.

Kvaček M (1973) Selenides from the uranium deposits of western Moravia, Czechoslovakia. Part 1. Berzelianite, umangite, eskebornite. Acta Univ Carol, Geol 1-2: 13-36

Kvaček M (1979) Selenides from the deposits of western Moravia, Czechoslovakia – part 2. Acta Univ Carol, Geol 1-2: 15-38

Lafuente B, Downs RT, Yang H, Stone N (2015) The power of databases: the RRUFF project. In: Highlights in Mineralogical Crystallography, T Armbruster and R M Danisi, eds. Berlin, Germany, W. De Gruyter, pp 1-30

Liu J, Xie H, Wang J, Feng C, Zhou G, Li Z (2005) The relationship between carbonaceous chert and selenium enrichment in the Yutangba selenium deposit, China. Mineral Deposit Research: Meeting the Global Challenge (Beijing): 1407-1410. Springer

Lutz HD, Müller B (1991) Lattice vibration spectra. LX-VIII. Single-crystal Raman spectra of marcasite-type iron chalcogenides and pnictides, FeX_2 (X=S, Se, Te; P, As, Sb). Phys Chem Minerals 18: 265-268

Menez J, Botelho NF (2017) Ore characterization and textural relationship among gold, selenide, platinum-group minerals and uraninite at the granite-related Buraco do Ouro gold mine, Cavalcante, central Brazil. Mineral Mag 81(3): 463-475

Paar WH, Sureda RJ, Brodtkorb MK (1996) Mineralogía de los yacimientos de selenio en La Rioja, Argentina. Krutaita, tyrrellita y trogtalita de Los Llantenes. Revista de la Asociación Geológica Argentina, 51(4): 304-312

Picot P, Johan Z (1982) Atlas of ore minerals. B.R.G.M. Orléans, 458 pp.

Pluskal O (1992) Československý uran. Uhlí a rudy 1: 259-267

Pouchou JL, Pichoir F (1985) „PAP" (phi-rho-z) procedure for improved quantitative microanalysis. In: Armstrong JT (ed) Microbeam Analysis. San Francisco Press, San Francisco: 104-106

Sager M (1994) Spurenanalytik des Selenes. In Analytiker-Taschenbuch: 258-308. Springer-Verlag Berlin/ Heidelberg

Sejkora J, Macek I, Škácha P, Pauliš P, Plášil J, Toegel V (2014) Výskyt asociace Hg a Tl selenidů na opuštěném uranovém ložisku Zálesí v Rychlebských horách (Česká republika). Bull mineral-petrolog Odd Nar Muz (Praha) 22(2): 333-345

Sejkora J, Mazuch J, Abert F, Šrein V, Novotná M (1997) Supergenní mineralizace uranového ložiska Slavkovice na západní Moravě. Acta Mus Moraviae, Sci nat 81: 3-24

Sejkora J, Plášil J, Litochleb J, Škácha P, Pavlíček R (2012) A selenide association with macroscopic umangite from the abandoned uranium deposit Zálesí, Rychlebské hory Mountains (Czech Republic). Bull mineral-petrolog Odd Nar Muz (Praha) 20(2): 187-196

Simon G, Essene EJ (1996) Phase relations among selenides, sulfides, tellurides, and oxides. I. Thermodynamic properties and calculated equilibria. Econ Geol 91: 1183-1208

Simon G, Kessler SE, Essene EJ (1997) Phase relations among selenides, sulfides, tellurides, and oxides. II. Application to selenide-bearing ore deposits. Econ Geol 92: 468-484

Škácha P, Sejkora J, Plášil J (2017) Selenide mineralization in the Příbram uranium and base-metal district (Czech Republic). Minerals 7(6), 91

Šouba M (1974) Mineralizace zlomových struktur slavkovického ložiska. Sbor geol Věd, ložis Geol Mineral 16: 129-164

Vogt H, Chattopadhyay T, Stolz HJ (1983) Complete first-order Raman spectra of the pyrite structure compounds FeS_2, MnS_2 and SiP_2. J Phys Chem Solids 44(9): 869-873